Impact of Phosphorothioate Substitutions on the Thermodynamic Stability of an RNA GAAA Tetraloop: An Unexpected Stabilization†

Thomas E. Horton, Melissa Maderia, and Victoria J. DeRose*

Department of Chemistry, Texas A&M University, College Station, Texas 77842-3012

Received January 21, 2000; Revised Manuscript Received May 1, 2000

ABSTRACT: This study analyzes the impact of phosphorothioate substitutions on the thermodynamic stability of a 12-nt RNA hairpin containing a $^{5'}$GAAA$^{3'}$ tetraloop. The thermodynamic consequences of stereospecific phosphorothioate substitutions 5′ to each adenosine in the loop region are measured using optical melting and calorimetry experiments. Surprisingly, a single stereospecific phosphorothioate substitution 5′ to the second adenosine of the tetraloop, R_p-A7, results in a stabilization corresponding to a $\Delta(\Delta G_{37°C})$ of approximately −2.9 kcal mol^{-1} (0.1 M NaCl) when compared with that of an unmodified sample. Five other phosphorothioate-substituted samples did not show significant thermodynamic differences in comparison with the unsubstituted samples. Addition of Mg^{2+} to all of the hairpins studied results in increased t_m's that are fit with a general electrostatic model to a dissociation constant of $K_d(Mg^{2+}) \sim 2-3$ mM (0.1 M NaCl). The R_p-A7 phosphorothioate-substituted hairpin showed an unusual decrease in t_m and apparent increase in enthalpy of unfolding upon addition of Cd^{2+}. These results may impact the interpretation of interference mapping experiments that use phosphorothioate substitutions to characterize RNAs in solution.

Phosphorothioate substitutions are increasingly being used as a tool to study interactions involving the phosphodiester backbone of RNA (*1*−*4*). A common use of phosphorothioate substitutions, in which a nonbridging oxygen of the phosphodiester is replaced by sulfur, is to predict site-specific interactions with cations by making use of the differing metal ion coordination preferences of sulfur versus oxygen (*5*, *6*). Phosphorothioates also are a critical component of most antisense methods (*7*) and are important in the investigation of stereospecific interactions in enzymatic systems (*8*, *9*).

Phosphorothioate interference experiments have been used to study metal interactions in several ribozymes. In these experiments, the effects of phosphorothioate substitutions on Mg^{2+}-dependent activities are monitored. Inhibition of Mg^{2+}-dependent activity and rescue by a more thiophilic metal such as Mn^{2+} or Cd^{2+} implicate the substituted oxygen as a metal binding site. One of the first examples of the use of these substitutions to investigate RNA activity was with the hammerhead ribozyme. The results of stereospecific phosphorothioate interference experiments at the cleavage site have been used to predict metal interactions with the *pro-R* position of the hammerhead phosphodiester backbone (*10*−*13*). Metal rescue effects also have been reported for phosphorothioate substitutions in the VS (*4*), group I intron (*14*), and group II intron (*15*) ribozymes. Studies on larger ribozymes have used phosphorothioate interference experiments to map interactions that are required for proper folding. Several positions in the group I intron have been shown to be sensitive to phosphorothioate substitutions with respect to folding interactions and have also shown metal rescue effects in conjunction with these modifications (*1*, *14*). Basu et al. (*16*) also have reported the use of phosphorothioate substitutions in the A platform of the P4−P6 domain in conjunction with 6-thioguanosine to identify a monovalent cation binding site whose substitution could be rescued with Tl^{+}. These studies reflect the potential utility of these substitutions when investigating structure and function in complex RNAs.

Despite their prolific use, the thermodynamic and structural implications of site-specific phosphorothioate substitutions in RNA are not well characterized. Substitution of a nonbridging phosphodiester oxygen with sulfur is proposed to lead to two local effects: (i) a change in the localization of negative charge from both oxygens in the phosphodiester to primarily the sulfur in the phosphorothioate (*17*) and (ii) weakening of hydrogen bond acceptor strength upon sulfur substitution (*18*). It is often assumed that these effects are localized to the substituted site and do not contribute significantly to the overall structure or stability of the RNA. Given this, phosphorothioate substitutions are generally considered to have few significant long-range effects on RNA structure or stability and to be ideal as probes for specific interactions.

The use of phosphorothioate-substituted DNA is common in antisense gene technologies (*7*), and several studies have investigated the relative stability of duplexes containing phosphorothioate-substituted DNA (SDNA). These studies have shown that, in general, both single and multiple phosphorothioate substitutions result in lower melting temperatures of SDNA−RNA and SDNA−DNA duplexes of moderate length with respect to the unsubstituted hybrid (*19*−*22*). The S_p isomer of the phosphorothioate is reported to be generally less destabilizing than the R_p isomer (*20*).

† This work was supported by the NSF (CAREER), the NIH (GM58096), and the Texas Higher Education Board Advanced Research Program. V.J.D. is a Cottrell Scholar of the Research Corporation.

* Corresponding author. Phone: 979-862-1401. Fax: 979-845-4719. E-mail: derose@mail.chem.tamu.edu.

10.1021/bi000141d CCC: $19.00
Published on Web 06/23/2000

NMR studies of SDNA−RNA and SDNA−DNA hybrids have demonstrated that in duplexes no large structural effects are caused by phosphorothioate substitutions (*22*−*24*). Two minor changes have been reported as a result of the modification: (i) a higher percentage of C3′-endo sugar conformations in an SDNA of an SDNA−RNA sample when compared to that of an unsubstituted sample (*22*) and (ii) a decrease in the relative base-pair lifetimes in an SDNA−DNA duplex in comparison with the unsubstituted sequence, consistent with the decrease in stability observed for these modified sequences (*23*). Gonzalez et al. (*24*) studied effects of a single stereospecific phosphorothioate substitution in an SDNA−RNA duplex and found a very small torsional angle change at the phosphodiester bond that contained the sulfur substitution. Analogous substitutions and the impact that these have on the structure and stability of RNA−RNA duplexes have not been systematically characterized.

In this study we explore the effects of single phosphorothioate substitutions in the loop region of $^{5'}$GAAA$^{3'}$ hairpins. The $^{5'}$GAAA$^{3'}$ hairpin is a member of the GNRA family of hairpins (N = any nucleotide, R = purine) whose unique structure in the loop region is proposed to grant enhanced stability over other tetraloop hairpins (*25*). The increased stabilization of this tetraloop is believed to be due to hydrogen bonding and stacking interactions, including interactions between the G5 and A8 nucleotides at the base of the loop (*26*, *27*). The A's in the loop are proposed to be well stacked, adding to the observed thermodynamic stability (*27*).

These well-defined tertiary interactions make the GA_3 hairpin a good model with which the thermodynamic effects of phosphorothioate substitutions at sites proposed to be involved in tertiary interactions can be measured. Here we explore the thermodynamic effects of single and multiple phosphorothioate substitutions in the loop region of two 12-nucleotide $^{5'}$GAAA$^{3'}$ hairpins. The influence of different phosphorothioate isomers and the thermodynamic effects of added Mg^{2+} and Cd^{2+} are reported.

MATERIALS AND METHODS

RNA Synthesis and Purification. WT GU and CG hairpins were prepared by in vitro transcription using T7 polymerase as previously described (*28*, *29*). Phosphorothioate substitutions were carried out according to Slim and Gait (*10*) by using ATPαS instead of ATP with a few modifications to improve transcription efficiency. Site-specific phosphorothioate-containing hairpins were purchased from Dharmacon Research (Boulder, CO) and the diastereomers separated using published protocols (*10*) on a C-18 column (Pharmacia). R_p and S_p assignments were made on the basis of snake venom phosphodiesterase cleavage assays using published procedures (*10*). Diastereomeric purity was >90%.

Thermal Denaturation Experiments. RNA thermal denaturation experiments were carried out on a Cary 1 double-beam UV−vis spectrometer equipped with a variable temperature controller. Samples were prepared as described by Horton et al. (*29*) in 5 mM triethanolamine and 100 mM NaCl, pH 7.8. Sample RNA concentrations were between 1 and 20 μM and prepared by heating to 90 °C for 90 s and then cooling on ice for 30 min. Divalent cations were added from concentrated stock solutions in water. Samples were then loaded at room temperature into sealed cuvettes and placed in the spectrometer, which equilibrates to 4 °C for 30 min before the experiment is started. Data were collected at 0.3 or 0.7 deg intervals from 4 to 100 °C as measured by a temperature probe inserted into a dummy cuvette containing the standard melting buffer.

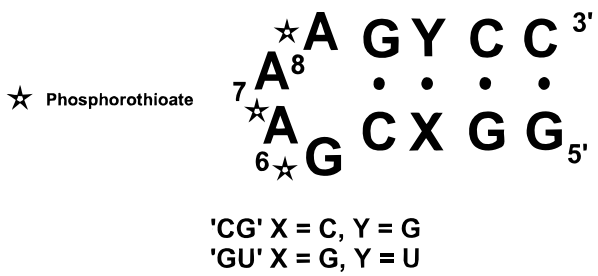

FIGURE 1: GAAA hairpins used in this study. Two stem sequences were studied and are denoted the CG and GU hairpins. Phosphorothioate substitutions, indicated by stars, are 5′ to each adenosine.

Analysis of Thermal Melting Profiles. Percent transmittance was recorded at 260 and 280 nm simultaneously. Data were converted from percent transmittance to absorbance and treated as previously described (*30*). The data sets were smoothed over a 4 °C window, and the melting profile was presented as the derivative of absorbance with respect to temperature and plotted as a function of temperature. The data presented here are fit to a sequential unfolding model described in detail previously (*30*). From measurements using different samples, representative errors associated with melting temperatures are ±0.5 °C with enthalpies varying by ±0.5−1 kcal mol^{-1} and calculated errors of ±0.8 kcal mol^{-1} for $\Delta G_{37°C}$.

Calorimetry Experiments. Differential scanning calorimetry (DSC) data were collected on a Microcal VP-DSC. RNA samples were prepared as previously described, degassed under vacuum, and loaded into a pressurized 500 μL sample cell at RNA concentrations between 30 and 60 μM. Samples were equilibrated to 1 °C for 30 min before the temperature was increased at the rate of 1 °C/min from 1 to 125 °C. Calorimetry data were analyzed using the program Origin (Microcal). A buffer baseline scan was subtracted from the raw DSC data. Following baseline correction, the data were fit to a sequential unfolding model as described by Theimer and Giedroc (*31*).

Analysis of Divalent Cation Concentration Dependence of the Melting Profiles. Mg^{2+} titration data were fit to the general equation derived by Laing et al. (*32*). This model assumes an electrostatic interaction of one Mg^{2+} ion for every two phosphates and two-state unfolding associated with the transition being fit (*32*, *33*). For the data presented here the number of phosphates involved in the unfolding process was held constant at four, and variation of this number between two and eight did not significantly affect the fits. The model generates, for a given unfolding transition, metal affinities for the folded form K_f and the unfolded form K_u (*33*).

RESULTS

The GAAA (GA_3) hairpins used in this study are depicted in Figure 1. GA_3 hairpins with two different stems were examined: the $^{5'}$GG**C**C(GA_3)G**G**CC$^{3'}$ ("CG") hairpin and a slightly destabilized $^{5'}$GG**G**C(GA_3)G**U**CC$^{3'}$ ("GU"). Both of the CG and GU hairpins were studied using wild-type (WT;

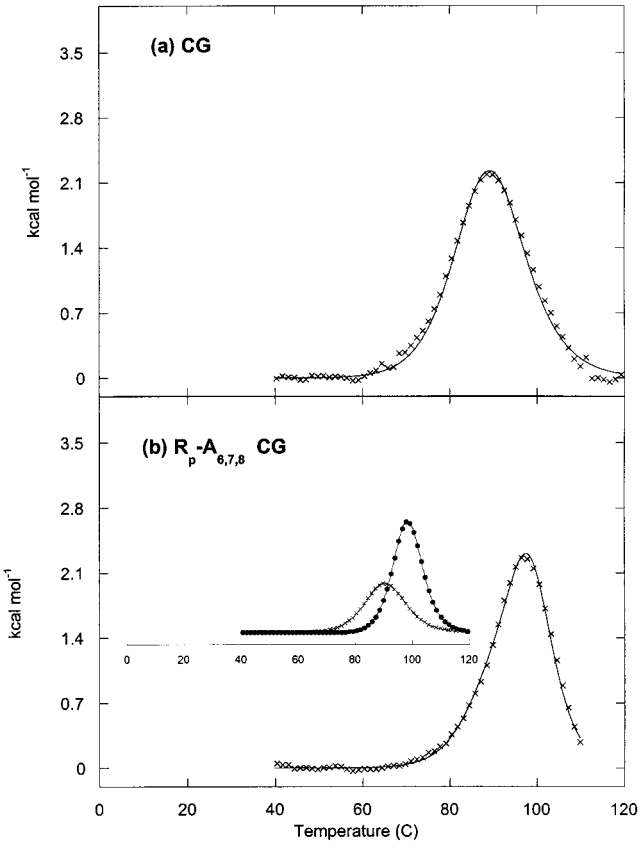

FIGURE 2: Differential scanning calorimetry (DSC) scans of the WT CG (a) and CG R_p-$A_{6,7,8}$ phosphorothioate-substituted hairpins (b). The inset in (b) represents the individual transitions that make up the total calculated fit to the raw data. The area under these curves was used to calculate ΔH as reported in Table 1.

all-phosphodiester backbone) and phosphorothioate-modified hairpins. The modified hairpins presented in this study consist of single or multiple phosphorothioate substitutions 5′ to the adenosines in the loop. Several substitutions were examined: a hairpin with R_p-phosphorothioates substituted 5′ to each of the adenosines (R_p-$A_{6,7,8}$) and the six diastereomeric hairpins substituted at individual sites, which include the R_p and S_p diastereomers 5′ to A6, A7, and A8.

Figure 2 shows differential scanning calorimetry data for the CG WT and the R_p-$A_{6,7,8}$ phosphorothioate-substituted hairpins. The t_m for the WT hairpin is 90 °C with an enthalpy of 48 kcal mol^{-1} in 0.1 M NaCl (Table 1), consistent with previous measurements for this stable tetraloop (*25*). The calorimetric scan for the CG hairpin containing three R_p-phosphorothioate substitutions, depicted in Figure 2b, shows an increase of ~8 °C in melting temperature. The large increase in t_m for these substitutions was surprising based on other observations for double-stranded SDNA−RNA models in which sulfur substitutions generally lead to a decrease in stability (*19*−*22*).

Unlike for the WT RNA, two transitions are required to fit the R_p-$A_{6,7,8}$ calorimetric data of Figure 2b. The two transitions (Figure 2b, inset) have t_m = 93 °C (ΔH_{cal} = 32 kcal mol^{-1}) and t_m = 99 °C (ΔH_{cal} = 23 kcal mol^{-1}) with ΔH_{total} slightly larger than that for the WT hairpin. Fitting these two transitions to a two-state van't Hoff model yielded calculated enthalpies much higher than those measured calorimetrically, which is consistent with non-two-state behavior for these transitions.

Table 1: Thermodynamics of Unfolding for 5′GAAA3′ Hairpins[a]

RNA	t_m (°C)	ΔH	$-\Delta G_{37°C}$	t_m (°C) 1 mM Mg^{2+}	ΔH	$-\Delta G_{37°C}$
CG[b]	89.5	48.2	7.0	90.8	52.0	7.7
R_p-$A_{6,7,8}$ CG[b,c]	92.9	31.9	4.9			
	98.9	23.1	3.8			
GU	62.7	38.2	2.9	66.4	37.6	3.3
R_p-$A_{6,7,8}$ GU[c]	71.9	19.3	2.0	78.2	16.9	1.9
	73.0	33.7	3.5	78.4	32.4	3.8
R_p-A6 GU	59.5	44.7	3.0	61.0	46.1	3.3
R_p-A7 GU	71.9	56.7	5.8	75.4	50.6	5.6
R_p-A8 GU	55.9	39.2	2.3	56.9	39.9	2.4
S_p-A6 GU	57.7	42.5	2.7	59.7	45.2	2.7
S_p-A7 GU	59.8	41.0	2.8	61.2	46.4	3.4
S_p-A8 GU	57.3	38.3	2.4	58.5	34.3	2.8
13-nt duplex[d]	77.3	82.3	9.5			
13-nt duplex R_p	78.8	96.9	11.5			
13-nt duplex S_p	75.4	85.5	9.4			

[a] Standard conditions: 5 mM triethanolamine and 100 mM NaCl, pH 7.8. ΔG and ΔH are reported in kcal mol^{-1}. The calculated error in ΔG is ±0.8 kcal mol^{-1}. [b] DSC measurements. [c] Derived from deconvolution of the calorimetric curve into two peak areas. These data do not exhibit two-state behavior. [d] 5′ACGGUC*GGUCGCC3′ (* = thio) hybridized as described in Materials and Methods with 5′GGCGACCGACCGU3′.

The high melting temperature of the CG hairpin makes it difficult to detect unfolding by optical methods. To observe the full transition optically, further studies were carried out on a hairpin that differed by a C-G to G-U substitution in the stem, reducing the t_m by ~25 °C (Figure 3a). Figure 3 shows the optical melting profiles for the GU WT and a series of phosphorothioate-substituted GU hairpins. The melting profiles are shown as the derivative of absorbance versus temperature detected at both 260 and 280 nm. The A_{260}/A_{280} ratio can aid in identifying the relative amounts of AU and GC character present in the RNA unfolding event (*34*). As observed with the CG hairpin, incorporation of three phosphorothioates 5′ to the adenosines again increased the overall observed t_m by approximately 9 °C (Figure 3b). As in the WT CG hairpin, two transitions are used to best fit the data (Figure 3b, inset).

To determine whether the stabilization observed for the phosphorothioate-substituted samples is due to an individual interaction or is a result of several interactions occurring in the loop, RNA hairpins with single phosphorothioate modifications 5′ to positions A6, A7, and A8 were examined (Figure 1). In each case, melting profiles of both the R_p and S_p diastereomers were obtained. Representative melting profiles are shown for the R_p-A7, S_p-A7, and R_p isomers of A6 and A8 in Figures 3, panels c and d, and S1, respectively. Of these samples, only the R_p-A7 hairpin exhibits the stabilization observed for the fully substituted R_p-$A_{6,7,8}$ hairpin. The inset in Figure 3c shows melts taken at 1 and 30 μM RNA concentrations (dots and crosses, respectively). The lack of change in the t_m between these samples demonstrates unimolecular behavior for this unfolding event, and this was observed for all hairpins in this study. The other substituted samples, including the S_p-A7 hairpin, did not exhibit a t_m increase in comparison with the unsubstituted hairpin (see Table 1). These data implicate the R_p-A7 phosphorothioate as primarily responsible for the enhanced stability in the R_p-$A_{6,7,8}$ phosphorothioate-substituted hairpin.

In Table 1, the t_m, unfolding enthalpies, and calculated values for $-\Delta G_{37°C}$ are tabulated for the various samples

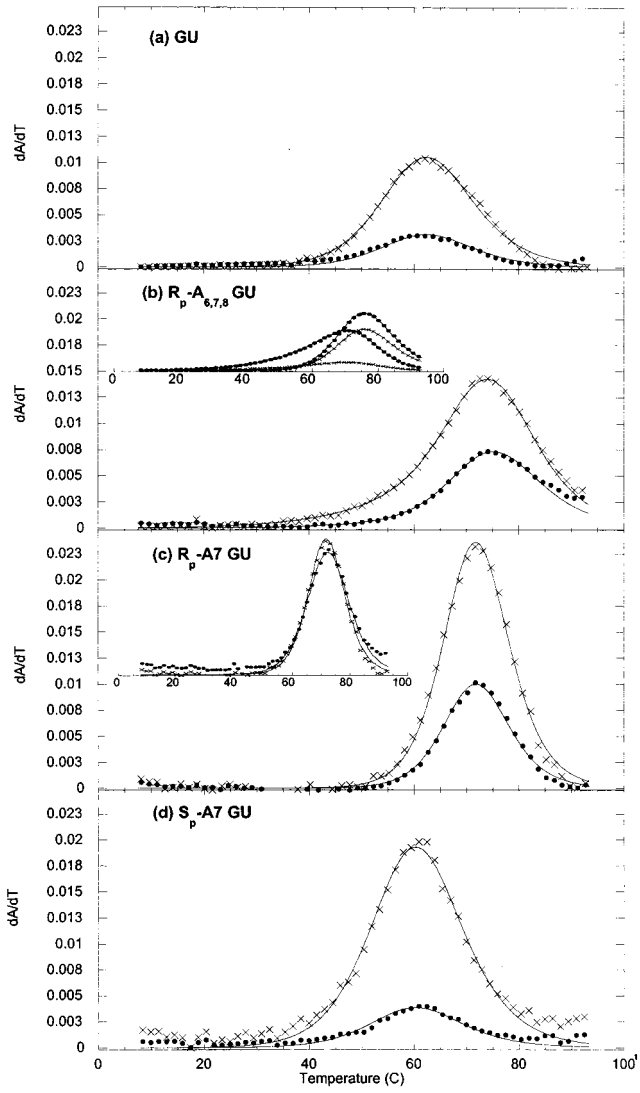

FIGURE 3: Comparison of representative optical melting profiles for the GU hairpin and phosphorothioate-substituted GU hairpins: (a) GU; (b) R_p-$A_{6,7,8}$ GU; (c) R_p-A7; (d) S_p-A7. The data were collected at two wavelengths [260 nM (●) and 280 nm (×)], and every fifth data point is plotted. The calculated fits are shown as continuous lines through each data set. The inset in (b) represents the individual transitions that make up the total calculated fit to the raw data at each wavelength. The inset in (c) compares two scans at 280 nm for two different R_p-A7 RNA concentrations of 1 μM (×) and 30 μM (●), for which the t_m's differ by less than 1 °C.

used in this study. For the multiple R_p-$A_{6,7,8}$ substitution, increased stabilities characterized by $\Delta(\Delta G_{37°C})$ of -1.7 and -2.6 kcal mol^{-1} are observed between substituted and WT samples for the CG and GU hairpins, respectively. The calculated difference in $\Delta G_{37°C}$ for the single GU R_p-A7 substitution versus the WT hairpin is -2.9 kcal mol^{-1}.

Both the R_p-A7 hairpin and the multiply substituted R_p-$A_{6,7,8}$ hairpins exhibit a characteristically higher A_{260}/A_{280} ratio of 0.5 in their melting profiles. All other hairpins exhibit similar and lower A_{260}/A_{280} ratios of approximately 0.3. A relative increase in absorbance at 260 nm can be indicative of increased A-U character in the folded RNA and may result from the stacking of an adenosine residue in the loop region that is stabilized by the R_p-A7 substitution.

Unlike all other hairpins in Table 1 which were best fit to one transition, the fits to the melting profiles of both the CG and GU R_p-$A_{6,7,8}$ phosphorothioate-substituted hairpins were substantially improved with two sequential transitions. The molecular significance of this deconvolution is unknown. It is reasonable to hypothesize that the two unfolding steps may involve the disruption of the helical stem and melting of the loop interactions. These melting profiles may, however, simply reflect non-two-state unfolding behavior (*33*) induced as a result of multiple sulfur substitutions. Similar, non-two-state behavior also has been observed in calorimetry measurements of DNA hairpin models (*35*).

Effect of Stereospecific Phosphorothioate Substitutions on a Duplex RNA. The thermodynamic properties of a 13-nt duplex RNA containing a single phosphorothioate substitution were measured to better understand the impact of a single sulfur substitution in a short A-form helix. The data in Table 1 show the results for three samples: a WT duplex and duplexes with single R_p or S_p phosphorothioate substitutions in the center of one strand. The results indicate a slight stabilization of the R_p-phosphorothioate-substituted hybrid (Table 1).

Effect of Divalent Cations on Hairpin Stability. Phosphorothioate substitutions are often used to probe for metal sites in RNA molecules, with a typical experiment measuring differences in activity in the presence of Mg^{2+} versus a more thiophilic metal such as Mn^{2+} or Cd^{2+}. It is therefore of interest to measure the effect of divalent metals on the stability of the phosphorothioate-substituted hairpins described above. The right-hand columns of Table 1 include the effect of 1 mM Mg^{2+} on the measured t_m's and enthalpies for the various hairpins studied, and Figure 4b shows a representative melting profile for the GU R_p-A7 hairpin in the presence of Mg^{2+}. As expected, addition of Mg^{2+} results in a small increase in t_m and enthalpy of unfolding for all of the hairpins. Using a nonspecific electrostatic binding model to fit titration data for the individual hairpins (*32*, *33*), binding constants for Mg^{2+} to the folded and unfolded forms of the hairpins were found to be $K_f \sim 500-700$ M^{-1}and $K_u \sim 200-300$ M^{-1}. A representative fit to the data is shown in Figure 5a for the R_p-A7 hairpin. These affinities are typical for nonspecific metal−RNA interactions in 0.1 M monovalent cation (*32*, *33*, *36*).

To characterize the effects of a "softer", more thiophilic metal on the sulfur-substituted RNA hairpins, Cd^{2+} titrations were carried out. The effect of Cd^{2+} on the R_p-A7 GU hairpin melting profile is shown in Figure 4c. In contrast to the effect of Mg^{2+}, a slight decrease in t_m is observed upon addition of Cd^{2+} to the R_p-A7 sample. At the same time, the derivative feature is seen to sharpen, suggesting a significant increase in the enthalpy of unfolding. Similar effects are observed for the R_p-$A_{6,7,8}$ hairpin (Figure 4d). These results are unusual for addition of divalent cations to RNA and indicate an unusual interaction between the R_p-A7 sample and the Cd^{2+} ion. The decrease in t_m is observed over a range of 0.1−1 mM Cd^{2+} for the R_p-A7 hairpin (Figure 5b).

In contrast to the R_p-A7 sample, the other phosphorothioate-substituted hairpins, including the S_p-A7 hairpin, exhibit t_m's that increase with low concentrations of Cd^{2+}, as expected for duplex RNA. At concentrations above 250 μM Cd^{2+}, however, the melting profiles of these RNAs began to show several nonhyperchromic features, with the lowest appearing at approximately 40 °C (data not shown). These features in the thermal denaturation data are coincident with

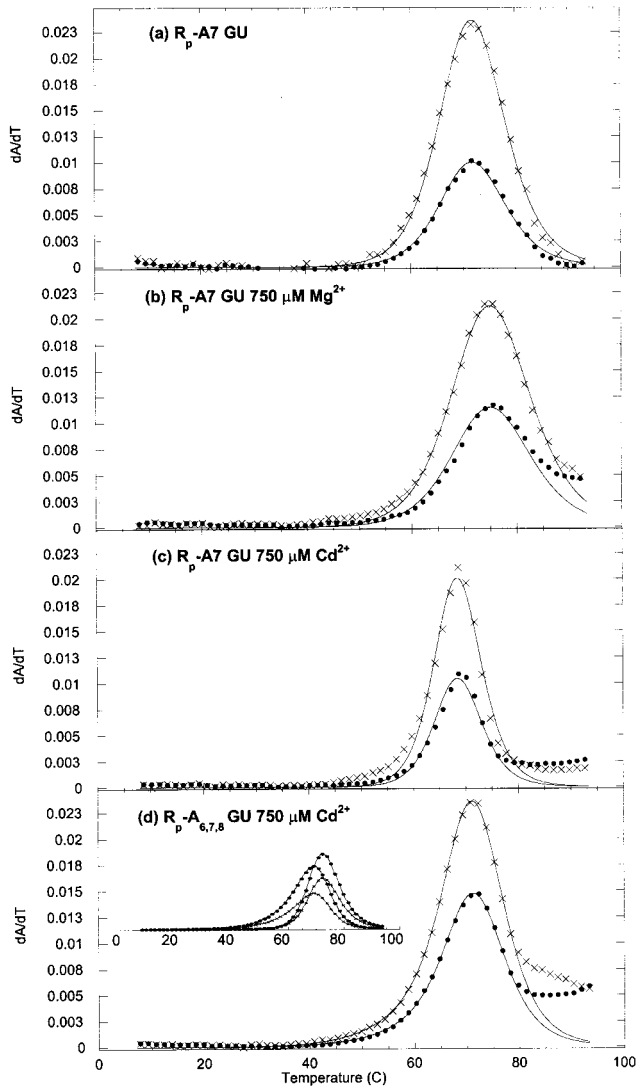

FIGURE 4: Effect of added metal on thermal denaturation profiles of R_p-$A_{6,7,8}$ and R_p-A7 hairpins: (a) R_p-A7 with no added metal; (b) R_p-A7 with 750 μM Mg^{2+}; (c) R_p-A7 with 750 μM Cd^{2+}; (d) R_p-$A_{6,7,8}$ with 750 μM Cd^{2+}. The inset in (d) represents the individual transitions that make up the total calculated fit to the raw data at 260 nm (●) and 280 nm (×).

the appearance of degradation products for the hairpins observed by HPLC (data not shown). Interestingly, no such features were observed in the melting profiles of either the R_p-A7 or the R_p-$A_{6,7,8}$ sample in Cd^{2+} concentrations up to 1 mM (data not shown).

In summary, phosphorothioate substitutions in the GA_3 tetraloop appear to have little impact on the stabilization of the hairpin structure induced by the nonspecific binding of Mg^{2+}. Most of the phosphorothioate substitutions, however, resulted in sensitivity to cleavage in low concentrations of thiophilic Cd^{2+} and at temperatures of approximately 40 °C. An R_p-phosphorothioate in the A7 position and the R_p-$A_{6,7,8}$ substituted hairpin show unusual thermodynamic effects upon addition of Cd^{2+} and are much less sensitive to Cd^{2+}-induced cleavage.

DISCUSSION

In this study we have investigated the thermodynamic effects of individual phosphorothioate substitutions on a common RNA structural motif, the $^{5'}$GAAA$^{3'}$ hairpin. It is

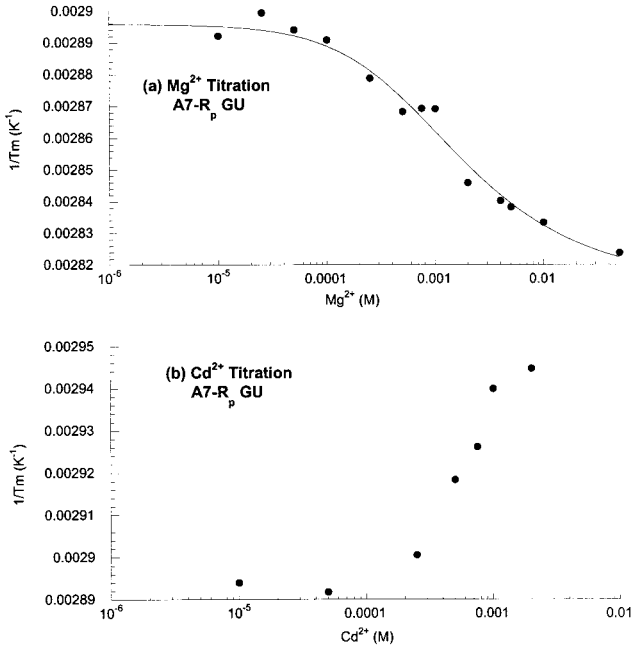

FIGURE 5: (a) Effect of Mg^{2+} on the t_m for the unfolding of the R_p-A7 substituted hairpin. The continuous curve through the data set represents a nonlinear least-squares fit assuming an electrostatic interaction as previously described (*32*, *33*). (b) Effect of Cd^{2+} on the t_m for the unfolding of the R_p-A7 substituted hairpin showing an unusual decrease in the measured t_m with added metal.

clear from the data presented here that the substitution of a sulfur for an oxygen in the *pro-R* position 5′ to A7 imparts a significant thermodynamic stabilization to the GAAA hairpin. For the GU hairpin with a single phosphorothioate substitution at A7, the stabilization is characterized by a higher melting temperature (+9.2 ± 0.4 °C) and enthalpy (+18.5 ± 0.9 kcal mol^{-1}), giving a $\Delta(\Delta G_{37°C})$ of −2.9 kcal mol^{-1} when compared to that of the WT sequence (Table 1). By contrast, the S_p substitution at this site and other substitutions 5′ to A6 and A8 in the tetraloop have very little thermodynamic effect on the stability of the tetraloop.

Hairpins with "stable" GNRA and UNCG loop sequences have previously been characterized thermodynamically (*25*, *37*−*39*). The effects of stable loop sequences are to significantly decrease the energetic penalty associated with loop closing of the RNA duplex. Antao and Tinoco reported ΔG contributions for loop formations (ΔG_{loop}) ranging from +1 kcal mol^{-1} for a stable UUCG loop to approximately +6 kcal mol^{-1} for an unstructured CCCC loop [in 1 M NaCl (*37*)]. Here we find ΔG_{loop} = +2.2 kcal mol^{-1} for the unmodified GU GAAA hairpin (0.1 M NaCl, 1 mM Mg^{2+}; Table 2). This calculation is done by comparing the results in Table 1 with ΔG values calculated for the four base-pair duplex (1 M NaCl) in the absence of a closing loop, assuming no interactions between the loop and stem (Table 2) (*40*). A similar value of ΔG_{loop} = +3.1 kcal mol^{-1} (1 M NaCl) can be calculated from data reported by Antao et al. (*25*) for an unmodified GAAA hairpin.

A striking difference is found in R_p-A7 and R_p-$A_{6,7,8}$ phosphorothioate-substituted hairpins. The ΔG_{loop} calculated for these RNAs is −0.1 and −0.2 kcal mol^{-1}, respectively, indicating that the phosphorothioate-substituted loop imparts a net *stabilization* of the four base-pair duplex stem with enthalpic gain overcoming the entropic cost for loop closure

Table 2: Calculated Free Energies of Loop Formation for WT and Phosphorothioate-Substituted Tetraloops

hairpin	$\Delta G_{37°C\ loop}$[a] (kcal mol^{-1})	hairpin	$\Delta G_{37°C\ loop}$[a] (kcal mol^{-1})
CG WT	+2.2	R_p-A7	−0.1
CG R_p-$A_{6,7,8}$	+0.5	S_p-A7	+2.1
GU WT	+2.2	R_p-A6	+2.2
GU R_p-$A_{6,7,8}$	−0.2	R_p-A8	+3.1

[a] Calculated using the experimental values for $\Delta G_{37°C}$ in Table 1 (100 mM NaCl, 1 mM Mg^{2+}) and subtracting a value of $\Delta G_{37°C\ stem} = -5.5$ kcal mol^{-1} [1 M NaCl, calculated for the 4 bp stem as in Antao and Tinoco (*37*)]. CG loop ΔG's were calculated using the values in the absence of 1 mM Mg^{2+} with $-\Delta G_{37°C\ stem} = -9.2$ kcal mol^{-1}.

(Table 2). This is a net stabilization of −2.3 kcal mol^{-1} (0.1 M NaCl, 1 mM Mg^{2+}) between the unsubstituted and the single atom substituted tetraloop.

It is of interest to speculate on structural changes that might cause the observed thermodynamic stabilization. The main interactions believed to be stabilizing the loop are hydrogen bonds extending the stem via a G-A base pair and stacking of the adenosines (*26*, *27*). On the basis of this structure, a sulfur substitution at the *pro-S* position 5′ to A8 should weaken a hydrogen bond predicted for this position, resulting in a loss in stability. However, previous studies suggest that an alternate hydrogen-bonding network may exist which could compensate for such a mutation, making its net thermodynamic contribution small (*27*, *38*). Consistent with this suggestion, comparison of stabilities of the S_p-A8, R_p-A8, and WT GU hairpins shows only small changes of ≤0.6 kcal mol^{-1} in $\Delta G_{37°C}$; these are within error of the current measurements.

The current structures give little insight into how the R_p-A7 substitution might stabilize the hairpin. The significant change observed in the A_{260}/A_{280} ratio is consistent with additional A-U character in the unfolding transition (*34*), possibly indicating a more stable stacking interaction between the adenosines in the tetraloop when the A7 *pro-R* position is substituted with a sulfur. How the phosphorothioate substitution might invoke this additional stacking is unclear. An alternative possibility is that the R_p-A7 substitution stabilizes duplex formation over that of the hairpin, but the concentration independence of the thermal denaturation profile argues against a bimolecular interaction as would be expected in duplex formation (Figure 3c inset).

As described in the accompanying paper (*41*), ^{31}P NMR spectroscopy has been used to monitor the effects of divalent cations on the structure of these substituted hairpins. Consistent with the thermodynamic data presented here, the ^{31}P NMR spectra of the R_p-A7 phosphorothioate-substituted sample suggests a unique structure for the substituted hairpin loop. The metal binding properties of the R_p-A7 hairpin, as observed by NMR, are also readily distinguished from those of the WT and other substituted hairpins. In the WT hairpin a Mg^{2+} ion is proposed to bind to the phosphodiester 5′ to A7. This binding is accompanied by perturbations in the A6 and G5 ^{31}P resonances which may be part of the binding pocket. The A7 phosphorothioate-substituted samples bind Cd^{2+} in place of Mg^{2+}, as expected, but only the S_p-A7 phosphorothioate shows accompanying effects at A6/G5 whereas the R_p-A7 sample exhibits no such changes. The Mg^{2+}-dependent thermodynamic data presented here are adequately fit with a nonspecific electrostatic model, and so a metal binding to a specific location in the hairpin does not appear to contribute a great deal of stability to the folded molecule. The unusual effects of Cd^{2+} on the thermodynamic data for the R_p-A7 sample are consistent, however, with the NMR observations that a unique metal binding environment exists upon substitution of the R_p-A7 oxygen with a sulfur.

The observed stabilization for the R_p-A7 phosphorothioate substitution of $\Delta(\Delta G_{37°C}) = -2.9$ kcal mol^{-1} (0.1 M NaCl) is significant and has some possible implications for the use of these substitutions in investigating structured RNAs. Reports by Laing and Draper yield free energy values associated with tertiary structure in the 58-nt domain of *Escherichia coli* rRNA to be between $\Delta G_{25°C} \sim 1.5-7$ kcal mol^{-1} (100 mM KCl) (*42*). Nixon and Giedroc have reported values for tertiary structure in a 28-nt pseudoknot of $\Delta G_{37°C} = -3.3$ kcal mol^{-1} (100 mM KCl) (*43*). Free energy values have also been reported for the ribose "zipper" in the P4−P6 domain in which each "tooth" in the zipper contributes $\Delta G_{37°C} \sim 1$ kcal mol^{-1} (10 mM NaCl) to the stability of the RNA (*44*).

Given the relatively large stabilization observed in the GA_3 tetraloop hairpin by substitution of a single phosphate oxygen, these results point at the potential of phosphorothioate substitutions to stabilize alternative structures in other RNA systems, which may be inactive due to misfolding rather than interference at a single site. Of the six substitutions investigated, one is found to significantly alter the hairpin unfolding characteristics, impacting both stability and metal binding properties (*41*) of this simple hairpin. It is clear that caution must be exercised in analyzing phosphorothioate interference experiments.

NOTE ADDED IN PROOF

Relevant to this work, a recently published NMR study (*45*) reports significant conformational changes associated with single phosphorothioate substitutions in an RNA hairpin.

ACKNOWLEDGMENT

We thank Dr. David P. Giedroc for the use of his instrumentation including the DSC supported by the NIH (Grant GM42569) and for helpful discussion. Mr. Paul Nixon and Dr. Jon Christopher developed the computer algorithms and fitting program for the optical data.

SUPPORTING INFORMATION AVAILABLE

Figure S1 containing melting profiles for the R_p-A6 and R_p-A8 phosphorothioate-substituted GU hairpins. This material is available free of charge via the Internet at http://pubs.acs.org.

REFERENCES

1. Eckstein, F., and Gindl, H. (1970) *Eur. J. Biochem. 13*, 558−564.
2. Christian, E. L., and Yarus, M. (1992) *J. Mol. Biol. 228*, 743−758.
3. Ruffner, D. E., and Uhlenbeck, O. C. (1990) *Nucleic Acids Res. 18*, 6025−6029.
4. Sood, V. D., Beattie, T. L., and Collins, R. A. (1998) *J. Mol. Biol. 282*, 741−750.
5. Jaffe, E. K., and Cohn, M. (1978) *J. Biol. Chem. 253*, 4823−4825.

6. Pecoraro, V. L., Hermes, J. D., and Cleland, W. W. (1984) *Biochemistry 23*, 5262−5271.
7. Mol, J. N., and Van Der Krol, A. R., Eds. (1991) *Antisense Nucleic Acids and Proteins*, Marcel Dekker, New York.
8. Connoly, B. A., Potter, B. V. L., Eckstein, F., Pingoud, A., and Grotjahn, L. (1984) *Biochemistry 23*, 3443−3453.
9. Eckstein, F. (1985) *Annu. Rev. Biochem. 54*, 367−402.
10. Slim, G., and Gait, M. J. (1991) *Nucleic Acids Res. 19*, 1183−1188.
11. Dahm, S. C., and Uhlenbeck, O. C. (1991) *Biochemistry 30*, 9464−9469.
12. Scott, E. C., and Uhlenbeck, O. C. (1999) *Nucleic Acids Res. 27*, 479−484.
13. Zhou, D., and Taira, K. (1998) *Chem. Rev. 98*, 991−1026.
14. Christian, E. L., and Yarus, M. (1993) *Biochemistry 32*, 4475−4480.
15. Boudvillain, M., and Pyle, A. M. (1998) *EMBO J. 17*, 7091−7104.
16. Basu, S., Rambo, R. P., Strauss-Soukup, J., Cate, J. H., Ferre-D'Amare, A. R., Strobel, S. A., and Doudna, J. A. (1998) *Nat. Struct. Biol. 5*, 986−992.
17. Frey, P. A., and Sammons, R. D. (1983) *Science 228*, 541−545.
18. Rablen, P. R., Lockman, J. W., and Jorgensen, W. L. (1998) *J. Phys. Chem. A 102*, 3782−3797.
19. LaPlanche, L. A., James, T. L., Powell, C., Wilson, W. D., Uznanski, B., Stec, W. J., Summers, M. F., and Zon, G. (1986) *Nucleic Acids Res. 14*, 9081−9093.
20. Kanehara, H., Wada, T., Mizuguchi, M., and Makino, K. (1996) *Nucleosides Nucleotides 15*, 1169−1178.
21. Kanaori, K., Tamura, Y., Wada, T., Nishi, M., Kanehara, H., Morii, T., Tajima, K., and Makino, K. (1999) *Biochemistry 38*, 16058−16066.
22. Bachelin, M., Hessler, G., Kurz, G., Hacia, J. G., Dervan, B., and Kessler, H. (1998) *Nat. Struct. Biol. 5*, 271−276.
23. Jaroszewski, J. W., Clausen, V., Cohen, J. S., and Dahl, O. (1996) *Nucleic Acids Res. 24*, 829−834.
24. Gonzalez, C., Stec, W., Reynolds, M. A., and James, T. L. (1995) *Biochemistry 34*, 4969−4982.
25. Antao, V. P., Lai, S. Y., and Tinoco, I. (1991) *Nucleic Acids Res. 19*, 5901−5905.
26. Heus, H. A., and Pardi, A. (1991) *Science 253*, 191−194.
27. Jucker, F. M., Heus, H. A., Yip, P. F., Moors, E. H. M., and Pardi, A. (1996) *J. Mol. Biol. 264*, 968−980.
28. Milligan, J. F., and Uhlenbeck, O. C. (1989) *Methods Enzymol. 180*, 51−62.
29. Horton, T. E., Clardy, D. R., and DeRose, V. J. (1998) *Biochemistry 37*, 18094−18101.
30. Theimer, C. A., Wang, Y., Hoffman, D. W., Krisch, H. M., and Giedroc, D. P. (1998) *J. Mol. Biol. 279*, 545−564.
31. Theimer, C. A., and Giedroc, D. P. (1999) *J. Mol. Biol. 289*, 1283−1299.
32. Laing, L. G., Gluick, T. C., and Draper, D. E. (1994) *J. Mol. Biol. 237*, 577−587.
33. Nixon, P. L., and Giedroc, D. P. (1998) *Biochemistry 37*, 16116−16129.
34. Fresco, J. R., Klotz, L. C., and Richards, E. G. (1963) *Cold Spring Harbor Symp. Quant. Biol. 28*, 83−90.
35. Vallone, P. M., Paner, T. M., Hilario, J., Lane, M. J., Faldasz, B. D., and Benight, A. S. (1999) *Biopolymers 50*, 425−442.
36. Schimmel, P. R., and Redfield, A. G. (1980) *Annu. Rev. Biophys. Bioeng. 9*, 181−221.
37. Antao, V. P., and Tinoco, I. (1992) *Nucleic Acids Res. 20*, 819−824.
38. SantaLucia, J., Kierzek, R., and Turner, D. H. (1992) *Science 256*, 217−219.
39. Tuerk, C., Gauss, P., Thermes, C., Groebe, D. R., Gayle, M., Guild, N., Stormo, G., D'Aubenton-Carafa, Y., Uhlenbeck, O. C., Tinoco, I., Brody, E. N., and Gold, L. (1988) *Proc. Natl. Acad. Sci. U.S.A. 85*, 1364−1368.
40. Turner, D. H., Sugimoto, N., and Freier, S. M. (1988) *Annu. Rev. Biophys. Biophys. Chem. 17*, 167−192.
41. Maderia, M., Horton, T. E., and DeRose, V. J. (2000) *Biochemistry 39*, 8193−8200.
42. Laing, L. G., and Draper, D. E. (1994) *J. Mol. Biol. 237*, 560−576.
43. Nixon, P. L., and Giedroc, D. P. (2000) *J. Mol. Biol. 296*, 659−671.
44. Silverman, S. K., and Cech, T. R. (1999) *Biochemistry 38*, 8691−8702.
45. Smith, J. S., and Nikonowicz, E. P. (2000) *Biochemistry 39*, 5642−5652.

BI000141D